Journal of Power Sources 185 (2008) 433–438

Contents lists available at ScienceDirect

Journal of Power Sources

journal homepage: www.elsevier.com/locate/jpowsour

Short communication

Planar air-breathing micro-direct methanol fuel cell stacks based on micro-electronic–mechanical-system technology

Jianyu Cao[a,b], Zhiqing Zou[a], Qinghong Huang[a], Ting Yuan[a,b], Zhilin Li[a], Baojia Xia[a], Hui Yang[a,*]

[a] Energy Science and Technology Laboratory, Shanghai Institute of Microsystem and Information Technology, Chinese Academy of Sciences, Shanghai 200050, China
[b] Graduate School of the Chinese Academy of Sciences, Beijing 100039, China

ARTICLE INFO

Article history:
Received 21 March 2008
Received in revised form 2 June 2008
Accepted 5 June 2008
Available online 21 June 2008

Keywords:
Micro-DMFC
Flow field
Stack
MEMS
Fuel distribution plate

ABSTRACT

To meet the demands for high power micro-electronic devices, two silicon-based micro-direct methanol fuel cell (μDMFC) stacks consisting of six individual cells with two different anode flow fields were designed, fabricated and evaluated. Micro-electronic–mechanical-system (MEMS) technology was used to fabricate both flow field plate and fuel distribution plate on the silicon wafer. Experimental results show that either an individual cell or a stack with double serpentine-type flow fields presents better cell performance than those with pin-type flow fields. A μDMFC stack with double serpentine-type flow fields generates a peak output power of ca. 151 mW at a working voltage of 1.5 V, corresponding to an average power density of ca. 17.5 mW cm^{-2}, which is ca. 20.7% higher than that with pin-type flow fields. The volume and weight of the stacks are only 5.3 cm^3 and 10.7 g, respectively. Such small stacks could be used as power sources for micro-electronic devices.

1. Introduction

The rapid development of portable electronic devices such as notebook computers, personal digital assistants (PDAs) and mobile telephones requires micro-power sources with high performance, long-lasting operating time and compact structure. Among potential candidates for micro-power sources, direct methanol fuel cells (DMFCs) provide significant advantages such as high energy density, low pollution, fewer safety concerns, rapid start-up and compactness over rechargeable batteries and other types of fuel cells for portable applications [1–4]. Much effort has been devoted to the development of the micro-direct methanol fuel cell (μDMFC) [5–9]. However, its performance still does not meet the requirements for practical applications.

Micro-flow fields into and out of which reactants are transferred and other components for fuel cells can be fabricated on a silicon wafer with high resolution and good reproducibility by using the micro-electronic–mechanical system (MEMS) technology. Thus, many researchers attempted to utilize MEMS technology to design and fabricate micro-fuel cells [7–10]. Kelley et al. [11] first reported a μDMFC with an active area of 0.25 cm^2 using a silicon wafer as the substrate. Subsequently, they reported a silicon-based mini-DMFC with a volume of 12 mm^3. Such a DMFC could deliver a peak power density of about 17 mW cm^{-2} with a forced air-flow on the cathode side at room temperature [12]. Lu et al. [13] developed a silicon-based μDMFC for portable applications. The single DMFC was assembled by sandwiching the membrane electrode assembly (MEA) between two micro-fabricated silicon plates. Using 2 or 4 M methanol on the anode and a forced air-flow on the cathode, a maximum power density of ca. 16 mW cm^{-2} was achieved at room temperature. Compared with the silicon substrate, the use of polymer could significantly simplify the fabrication process and reduce the total cost. An all-polymer μDMFC with a maximum power density of about 8 mW cm^{-2} was fabricated using MEMS technology by Cha et al. [14]. Another prominent character of MEMS fabrication technology is its convenience for integrating components and forming a compact μDMFC system for portable applications. Yao et al. [15] proposed a μDMFC system which contains a cell, a micro-pump for collecting water back to the anode, and a passive liquid–gas separator for CO_2 removal. All these components could be integrated on a silicon substrate to eliminate interconnections and to minimize packaging costs. For further practical applications, single fuel cells need to be connected together to form a stack to meet the voltage requirements and to ensure a high output power. However, no one has reported an integration of a μDMFC stack based on MEMS technology. Previous study showed that a miniature PEMFC stack with six individual fuel cells was fabricated by utilizing MEMS technology [16]. The maximum power density of this stack approaches 104 mW cm^{-2} at room temperature. However, hydrogen storage still remains a big challenge for practical applications of a micro-

* Corresponding author. Tel.: +86 21 32200534; fax: +86 21 32200534.
E-mail address: hyang@mail.sim.ac.cn (H. Yang).

0378-7753/$ – see front matter © 2008 Elsevier B.V. All rights reserved.
doi:10.1016/j.jpowsour.2008.06.033

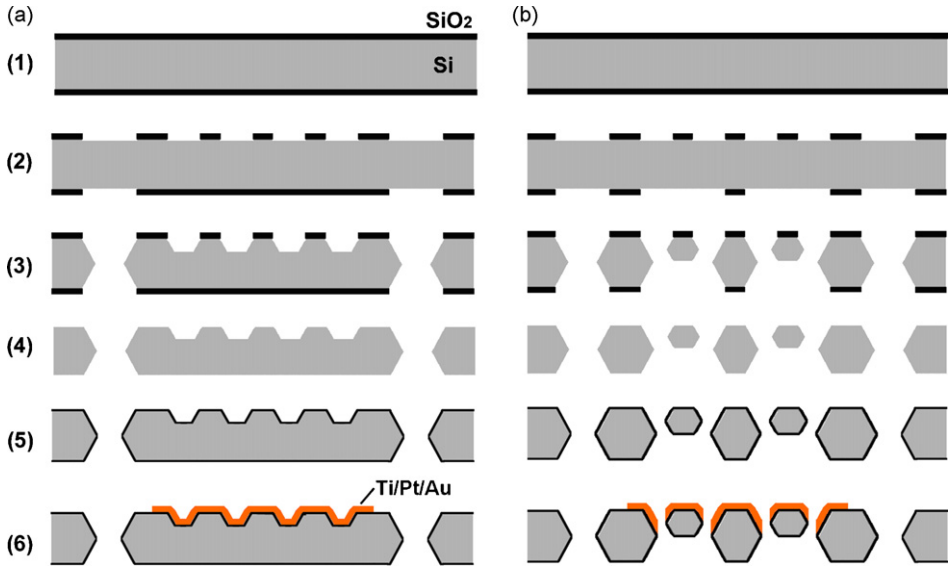

Fig. 1. MEMS fabrication process for both anode (a) and cathode (b) flow field plates for the μDMFC. (1) Thermal oxidation; (2) photolithography and dioxide etching on both sides; (3) silicon deep etching by 40 wt.% KOH solution; (4) residual SiO_2 etching by BOE solution; (5) second thermal oxidation; (6) sputtering a Ti/Pt/Au layer as a current collector.

PEMFC. Recently, Zhong et al. [17] presented a silicon-based μDMFC stack that consists of only two individual cells stacked one by one with the anode plate shared. Such a μDMFC stack generates a maximum power density of 12.71 mW cm^{-2}, which is higher than that of individual cell with a maximum power density of 9.12 mW cm^{-2}. However, the voltage and output power is still not high enough to meet expected application requirements especially with only stacking two cells.

Previously, Hsieh et al. [18,19] have investigated the effects of three different kinds of flow fields (i.e. interdigitated, serpentine and pin) on the cell performance of the μPEMFCs. It was found that that the μPEMFC with either an interdigitated-type or a serpentine-type flow field exhibits better cell performance than that with the pin-type flow field. Jung et al. [20] have reported the effects of cathode flow fields on the DMFC's performance and found that the DMFC with the serpentine-type structure at the cathode side presents better performance than that with the pin-type structure. However, the comparisons of the anode flow fields for both individual μDMFC and μDMFC stack have not been reported yet. In this work, two silicon-based μDMFC stacks consisting of six individual μDMFCs with different anode micro-flow fields were fabricated using MEMS technology. The performance of both individual DMFCs and stacks under air-breathing operating mode were evaluated and compared.

2. Experimental

2.1. MEMS fabrication of micro-flow field plates for μDMFCs

The micro-flow field plates of both the anode and cathode for μDMFCs were fabricated using a series of fabrication steps tailored from MEMS technology. Generally, the procedure includes using photolithography and KOH wet etching to form micro-channels and feed holes in a silicon wafer. The surface of the silicon wafers was then oxidized and deposited with a Ti/Pt/Au layer as current collectors. The MEMS fabrication process is described in Fig. 1.

Beginning with a 4 in. ⟨1 0 0⟩ oriented silicon wafer (P-type, 525 ± 20 μm thick) polished on both sides, a 2 μm silicon dioxide layer was grown by wet thermal oxidation. Then photolithography was used to define the flow channel geometry on the front side and the feed hole geometry on the rear side. The exposed oxide was removed by a buffered oxide etch (BOE), followed by anisotropic KOH etching down to a channel depth of approximately 270 μm. After the residue of previously coated SiO_2 was removed by a BOE, a new 2 μm silicon dioxide was grown as an insulator layer on the surface by wet thermal oxidation. Ti, Pt, and Au (200/2000/3000 Å in thickness, respectively) were subsequently sputtered on the channel surface as the current collectors. Finally, the wafer was diced into individual plates for fuel cell assembly.

2.2. Fabrication of a liquid fuel distribution plate

Parallel flow channels were designed to ensure uniform fuel distribution to each of 6-cell stack. Previously, a fuel distribution plate used to transfer and store hydrogen for the μPEMFC was fabricated [16]. However, considering the difference between liquid fuel (i.e.

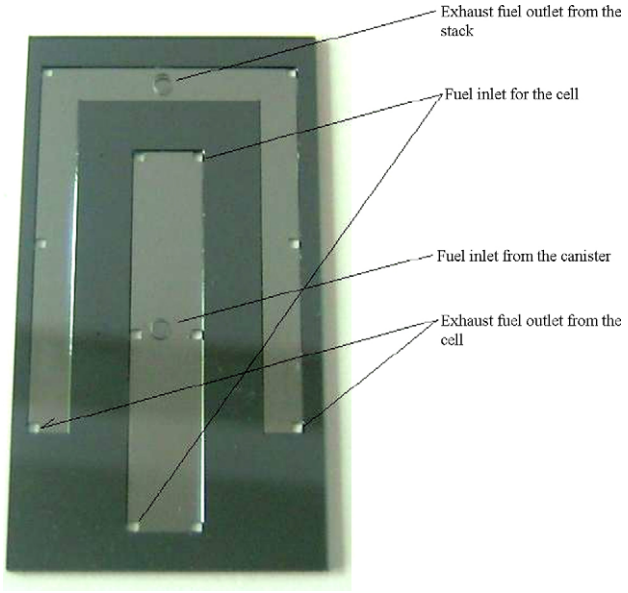

Fig. 2. A picture of the improved fuel distribution plate for the μDMFC stack.

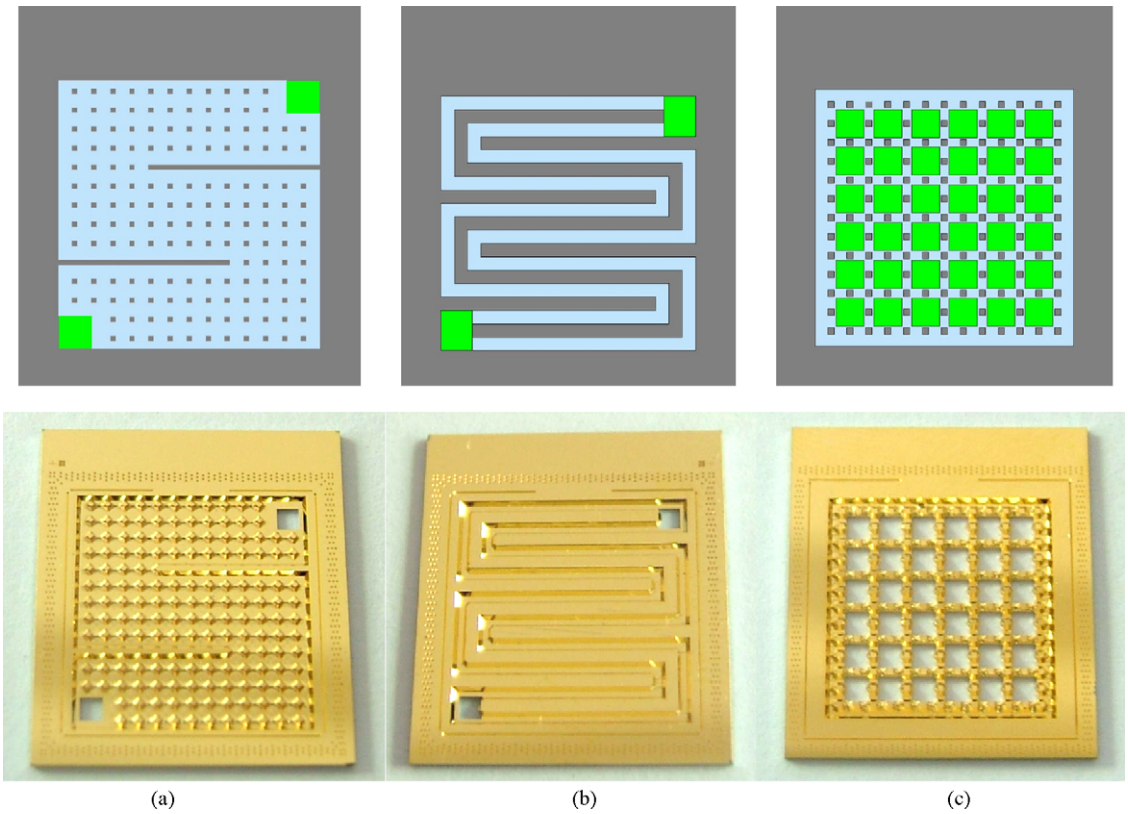

Fig. 3. The patterns of (a) pin-type anode flow field plate, (b) double serpentine-type anode flow field plate and (c) the through hole-type cathode flow field plate for the μDMFC.

methanol solution) and gaseous fuel (i.e. hydrogen), and convenient removal of the product (i.e. carbon dioxide), the fuel distribution plate was modified to meet the demand of the μDMFC stack. The depth of the chamber was about 270 μm, which is much deeper than that for hydrogen delivery. In addition, a Pyrex glass plate was bonded in front of the silicon wafer in order to assemble the stack conveniently.

The detailed fabrication procedure is shown as follows. First, using the wet etching method described above, a strip chamber of about 43 mm long, 7.9 mm wide and 270 μm deep and an U-type chamber of about 120 mm long, 4.4 mm wide and 270 μm deep were fabricated on a silicon wafer with a thickness of 525 μm. Second, a piece of Pyrex glass with a thickness of 500 μm was bonded with the silicon wafer together by using a silicon-glass bonding technique. Two holes with a diameter of 2.0 mm on the Pyrex glass were drilled before as the fuel inlet and outlet. The corresponding fuel inlets and outlets for each individual cell were square holes of about 1.44 mm × 1.44 mm. The picture of the fuel distribution plate for the μDMFC stack is shown in Fig. 2.

2.3. MEA preparation

A pretreated Nafion117 membrane was employed in this work. The pretreatment procedures include boiling the membrane in 3 vol.% H_2O_2 solution, washing with ultrapure water, boiling in 0.5 M H_2SO_4 solution and washing with ultrapure water for 2 h in turn. The pretreated membranes were kept in ultrapure water prior to the fabrication of MEAs.

Toray carbon paper (TGPH060, 20 wt.% PTFE, E-TEK Inc.) and carbon cloth (Type A, 20 wt.% PTFE, E-TEK Inc.) were used as the backing layers for the anode and cathode, respectively. A slurry which consisted of Vulcan XC-72 carbon and PTFE (25 wt.%) was coated onto carbon cloth to form a micro-porous layer (MPL) at the cathode side. Carbon-supported Pt (HiSPEC^{TM}9000, Johnson Matthey Inc.) and carbon-supported Pt–Ru (HiSPEC^{TM}10000, Johnson Matthey Inc.) were used as the catalysts for both cathode and anode, respectively. The MEA was prepared in the following manner. The catalyst ink was prepared by dispersing an appropriate amount of catalyst in a solution of ultrapure water, isopropyl alcohol, and 5 wt.% Nafion solution (Aldrich). The catalyst ink was then sprayed on the MPL. The catalyst loading was 6.0 ± 0.2 mg cm^{-2} for both cathode and anode, and the ionomer loading was 20 wt.% for cathode and 25 wt.% for anode, respectively. Finally, the MEA was prepared by hot pressing at 130 °C and 6 MPa for 3 min.

2.4. Assembly of μDMFC stacks

Prior to the assembly of the single fuel cell, the MEA was cut into six pieces each with a dimension of 1.4 cm × 1.4 cm. Then, each MEA piece was sandwiched between an anode plate and a cathode plate, and then pressed by an electronic spiral micrometer. An improved epoxy resin was used as a packaging material to assemble the μDMFC stack because of its chemical inertness to methanol and good stickiness and bonding strength. These assembled cells were mounted one by one on the rear side of the fuel distribution plate. Each cell was connected in series by spot welding the adjacent cells to make them electrically conductive. Finally, all the void space between the cells and fuel distribution plate was sealed with the epoxy resin to ensure no fuel leakage.

2.5. Performance evaluation

Both individual μDMFCs and μDMFC stacks were tested on an Arbin FCT system (Arbin Inc., USA). In this work, a 2 M methanol

Table 1
Dimension and internal resistance of individual μDMFCs and μDMFC stacks

Single or stack	Anode flow field	Dimension (mm^3)	Active area (mm^2)	Cell thickness (mm)	Internal resistance ($\Omega\,cm^2$)
M-1	Pin-type	14 × 18 × 1.6	144	1.60 ± 0.02	0.644 ± 0.014
M-2	Double serpentine	14 × 18 × 1.6	144	1.60 ± 0.02	0.530 ± 0.010
S-1	Pin-type	61 × 32 × 2.7	864[a]	2.70 ± 0.02	5.630 ± 0.120
S-2	Double serpentine	61 × 32 × 2.7	864[a]	2.70 ± 0.02	4.030 ± 0.144

[a] The sum of six individual cells' active area.

solution was used. A peristaltic pump with controllable flow rate ranging from 0.01 to 10 mL min^{-1} was used to deliver methanol aqueous solution. It is known that the fuel flow rate will have an influence on fuel cell's performance due to the mass transfer limitation, especially at low flow rate. However, at high flow rate, the effect of flow rate on cell's performance is negligible. In fact, if the flow rate is too high, the internal pressure of liquid will be rapidly increased, which will influence the stability of the DMFC performance and methanol crossover. For the stack, more methanol solution needs to be fueled since the total active area of the stack is much higher than that of the single cell. Typically, a flow flux of 0.2 mL min^{-1} was chosen for the single cells as well as a flow flux of 0.4 mL min^{-1} for the stacks. For each discharging current point along the polarization curve, a period of 1 min waiting time was used to obtain the stable voltage. The internal resistance of the μDMFC was measured using the Arbin FCT's built-in function [21]. When using this function, a transient current pulse is applied and followed by a constant-current charge or discharge step, which leads to changes in output voltage and current at that moment (ΔV and ΔI, respectively). The internal resistance is then calculated by $\Delta V/\Delta I$. For the performance evaluation, both single cells and stacks were placed in a thermostated container at a temperature of ca. 25 ± 1 °C.

3. Results and discussion

Two anodic micro-flow fields with different flow channel structures, i.e. double serpentine-type and pin-type, were designed and fabricated to investigate the effect of flow field structure on the performance of the μDMFCs. The pattern of the pin-type channel is shown in Fig. 3(a), which is an array of pin-type isolated "isles" with two through square holes for fuel in and out. The isle is about 300 μm × 300 μm on top and 270 μm in depth and the through holes for fuel in and out are about 1.5 mm × 1.5 mm. The pattern of the double serpentine-type channel is shown in Fig. 3(b), in which the channel is 120.0 mm long, 633 μm wide and 270 μm deep. The pattern of the cathode flow field used is shown in Fig. 3(c), which is through hole-type channels. For a typical cathode flow field, there is an array of micro-columns on the front side which will contact the MEA as the current collectors, and through holes between the columns which will be used for air-breathing. These columns are about 300 μm × 300 μm on top and 270 μm in depth and all through holes are about 1.2 mm × 1.2 mm. The dimension of a single flow field plate is about 16 mm × 18 mm with an active area of 12 mm × 12 mm. For each plate, about 2 mm × 16 mm free spaces were used for spot welding between the adjacent cells.

Fig. 4 is a picture of the planar μDMFC stack. The detailed dimensions of the individual μDMFCs and the μDMFC stacks are listed in Table 1. The volume and weight of a μDMFC stack are only about 5.3 cm^3 and 10.7 g, respectively. In addition, in order to meet the requirements of practical applications, the entire assembly process can even include the integration of a micro-pump, a small canister and an electronic controller to form a prototype μDMFC system. The volume and weight of such a prototype μDMFC system are ca. 90 cm^3 and 42.3 g, respectively.

A dilute methanol solution of 2 M was usually used to fuel the μDMFCs in order to decrease the effect of methanol crossover. Fig. 5 shows the polarization curves of two individual μDMFCs under air-breathing mode at 25 ± 1 °C. The open circuit voltages (OCV) of the μDMFC (M-1) with a pin-type anode flow field and the μDMFC (M-2) with a double serpentine-type anode flow field are 0.722 and 0.690 V, respectively. In the low current density region, the two single μDMFCs exhibited similar kinetic and ohmic polarization behavior. However, when the current densities are higher than 80 mA cm^{-2}, the polarization curve of M-1 shows a large voltage drop due to mass transport limitation compared with that of M-2, demonstrating that the anode flow field structure has a significant influence on the mass transport of a DMFC. It is possible that a double serpentine-type micro-flow field can provide more homogeneous fuel distribution than a pin-type anode flow field, thus

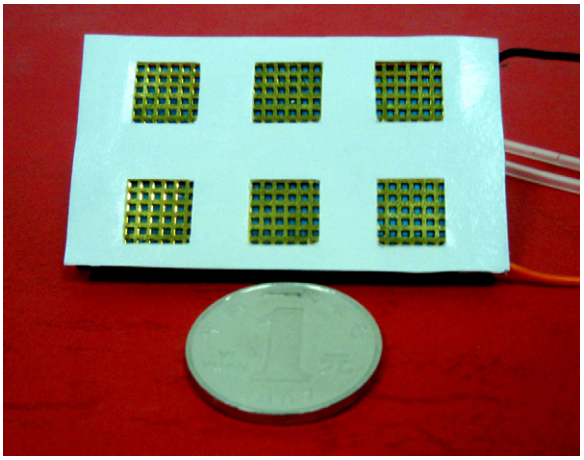

Fig. 4. A picture of the μDMFC stack.

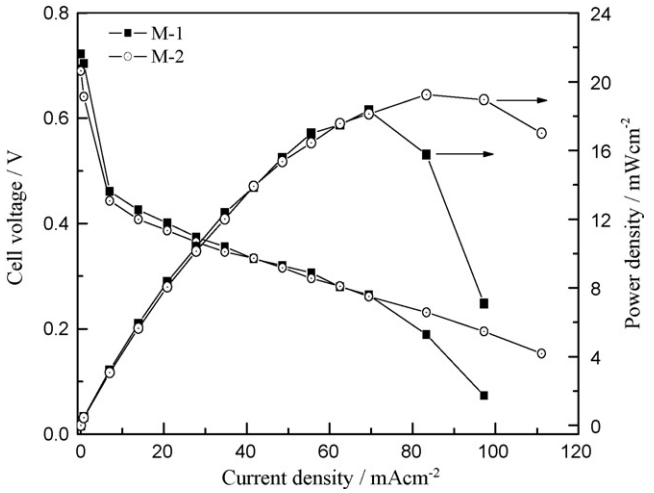

Fig. 5. Polarization curves of two individual air-breathing μDMFCs using a 2 M methanol solution with a flow flux of 0.2 cm^3 min^{-1} at 25 ± 1 °C.

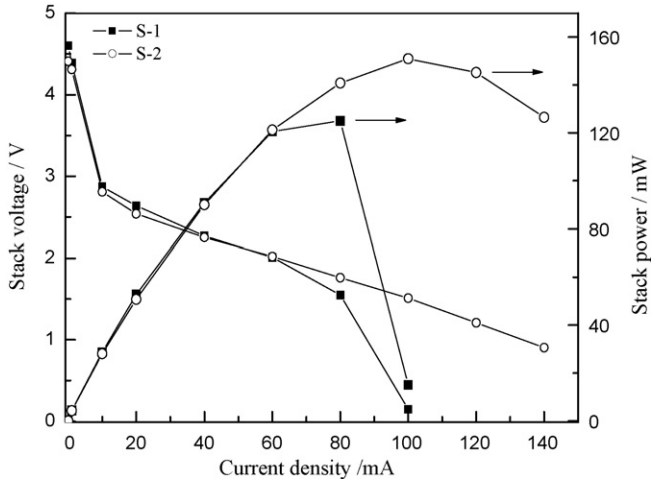

Fig. 6. Polarization curves of two μDMFC stacks under air-breathing mode using 2 M methanol solution with a flow flux of 0.4 $cm^3\ min^{-1}$ at 25 ± 1 °C.

leading to an improvement in mass transport on the anode side, especially when operating under high current densities. The maximum power density of M-2 is about 19.3 mW cm^{-2}, which is higher than that of M-1 of 18.3 mW cm^{-2}. The obtained maximum power density in this work is also higher than previously reported results with a forced air-flow on the cathode side with peak power densities of ca. 17 and 16 mW cm^{-2}, respectively [12,13]. The internal resistances of two μDMFCs (both individual cell and stack) are provided in Table 1. It is clear that the internal resistance of M-2 is lower than that of M-1, suggesting that a double serpentine-type flow field provides a larger current collector area than a pin-type microflow field so that the contact resistance was decreased between the flow field plate and the anode gas diffusion layer. According to the dimensions of flow field patterns, the current contact areas of M-1 and M-2 are calculated as 0.24 and 0.65 cm^2, respectively.

Fig. 6 illustrates a performance comparison of two μDMFC stacks with two different flow fields, each with six individual μDMFCs. In the low current region, the two μDMFC stacks exhibited similar kinetic and ohmic polarization behavior. In the high current region, the mass transport limitation is clearly shown for the μDMFC stack (S-1) with the pin-type anode flow fields, similar to the result for the single μDMFC. Yet, for the stack (S-2) with the double serpentine-type flow fields, no obvious mass transport limitation was observed, suggesting that a double serpentine-type flow field is more appropriate to be used as the anode flow field for the μDMFC. The peak output power of S-1 is ca. 125 mW, corresponding to a power density of 14.5 mW cm^{-2}. For S-2, a peak output power of ca. 151 mW was obtained at a working voltage of 1.50 V, corresponding to a power density of about 17.5 mW cm^{-2}. The maximum power of S-2 is ca. 20.7% higher than that of S-1, again indicating that the double serpentine-type flow field is more suitable for the anode flow field in a DMFC. Both μDMFC stacks exhibited better performance than that of a two-cell stack provided with pure oxygen under similar operating conditions [17]. Internal resistances of two stacks as shown in Table 1 are much higher than the sum of corresponding individual cells, indicating that the assembly technology for the stacks needs to be further improved. The obtained power densities for the two μDMFC stacks are lower than those of the individual μDMFCs, probably due to the following reasons. The electro interconnection in the stack is not good as expected, which leads to large contact resistance among the individual cells. Another possible reason is that the fuel distribution in the stack is not uniform as that in single cell.

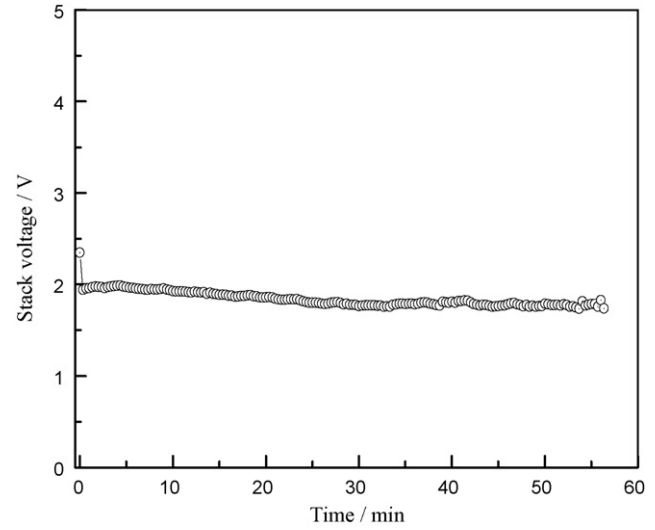

Fig. 7. Galvanostatic curve of a μDMFC stack with double serpentine-type anode flow field at a constant current of 57.6 mA (i.e. 40 mA cm^{-2}) under air-breathing mode using a 2 M methanol solution with a flow flux of 0.4 $cm^3\ min^{-1}$ at 25 ± 1 °C.

Fig. 7 shows the voltage of a μDMFC stack (S-2) at a constant current of 57.6 mA (i.e. 40 mA cm^{-2}) under air-breathing mode at 25 ± 1 °C. It can be seen that such a stack can provide a steady-state power output of about 110 mW for more than 50 min without significant degradation.

4. Conclusion

In summary, the study on the effect of anode flow field structures on the performance of either an individual μDMFC or a μDMFC stack reveals that the utilization of the double serpentine-type flow field significantly improves the mass transport of a μDMFC. The maximum power density of an individual DMFC with double serpentine-type flow field is ca. 19.3 mW cm^{-2} under an air-breathing mode at a temperature of ca 25 °C. Whereas a μDMFC stack with the double serpentine-type flow fields generates a peak output power of ca. 151 mW, which is ca. 20.7% higher than that with pin-type flow fields. The technology used here could be extended by integrating more individual cells into a stack to meet the demands for higher power electronic devices.

Acknowledgments

We would like to thank the National “863” High-Technology Research Programs of China (2006AA05Z136, 2006AA04Z342, 2007AA05Z141, 2008AA05Z102), the National Natural Science Foundation of China (20706056), the 100 People Plan Program of the CAS and the Pujiang Program of Shanghai City (No. 06PJ14110) for support of this work.

References

[1] X. Ren, T.E. Springer, S. Gottesfeld, J. Electrochem. Soc. 147 (2000) 92–98.
[2] D. Kim, E.A. Cho, S.A. Hong, I.H. Oh, H.Y. Ha, J. Power Sources 130 (2004) 172–177.
[3] Z. Guo, A. Faghri, J. Power Sources 160 (2006) 1142–1155.
[4] Z. Guo, A. Faghri, J. Power Sources 160 (2006) 1183–1194.
[5] G.Q. Lu, C.Y. Wang, J. Power Sources 144 (2005) 141–145.
[6] A. Blum, T. Duvdevani, M. Philosoph, N. Rudoy, E. Peled, J. Power Sources 117 (2003) 22–25.
[7] Y. Yamazaki, Electrochim. Acta 50 (2004) 663–666.
[8] S. Motokawa, M. Mohamedi, T. Momma, S. Shoji, T. Osaka, Electrochem. Commun. 6 (2004) 562–565.
[9] Y. Zhang, J. Lu, S. Shimano, H. Zhou, R. Maeda, Electrochem. Commun. 9 (2007) 1365–1368.

[10] W.Y. Sim, G.Y. Kim, S.S. Yang, Proceedings of the 14th IEEE International Conference on MEMS, Tech. Digest, 2001, pp. 341–344.
[11] S.C. Kelly, G.A. Deluga, W.H. Smyrl, Electrochem. Solid State 3 (2000) 407–409.
[12] S.C. Kelly, G.A. Deluga, W.H. Smyrl, AIChE J. 48 (2002) 1071–1082.
[13] G.Q. Lu, C.Y. Wang, T.J. Yen, X. Zhang, Electrochim. Acta 49 (2004) 821–828.
[14] H.Y. Cha, H.G. Choi, J.D. Nam, Y. Lee, S.M. Cho, E.S. Lee, J.K. Lee, C.H. Chung, Electrochim. Acta 50 (2004) 795–799.
[15] S.C. Yao, X. Tang, C.C. Hsieh, Y. Alyousef, M. Vladimer, G.K. Fedder, C.H. Amon, Energy 31 (2006) 636–649.
[16] X. Zhang, D. Zheng, T. Wang, C. Chen, J. Cao, J. Yan, W. Wang, J. Liu, H. Liu, J. Tian, X. Li, H. Yang, B. Xia, J. Power Sources 166 (2007) 441–444.
[17] L. Zhang, X. Wang, Y. Jiang, Q. Zhang, X. Qiu, Y. Zhou, L. Liu, Sens. Actuators A 143 (2008) 70–76.
[18] S.S. Hsieh, S.H. Yang, J.K. Kuo, C.F. Huang, H.H. Tsai, Energy Conv. Manage. 47 (2006) 1868–1878.
[19] S.S. Hsieh, S.H. Yang, C.L. Feng, J. Power Sources 162 (2006) 262–270.
[20] G.B. Jung, A. Su, C.H. Tu, Y.T. Lin, F.B. Weng, S.H. Chan, J. Power Sources 171 (2007) 212–217.
[21] J.G. Liu, T.S. Zhao, R. Chen, C.W. Wong, Electrochem. Commun. 7 (2005) 288–294.